

Kinetics of Sphalerite leaching by Sodium Nitrate in Sulfuric Acid

M. Hasani, S.M.J. Koleini and A. Khodadadi*

Mining Engineering Department, Tarbiat Modares University, Tehran, Iran

Received 1 July 2014; received in revised form 2 March 2015; accepted 4 May 2015

*Corresponding author: akdarban@modares.ac.ir (A. Khodadadi).

Abstract

In the present work, the extraction of zinc from a sphalerite concentrate using sodium nitrate as an oxidant in a sulfuric acid solution was investigated. The effective parameters such as the temperature, sulfuric acid and sodium nitrite concentrations, stirring speed, particle size, and solid/liquid (S/L) ratio were analyzed. The dissolution rate increased with increase in the sulfuric acid and sodium nitrite concentrations and temperature but decreased with increase in the particle size and S/L ratio. Moreover, the stirring speed had a significant effect on the leaching rate. Under the optimum conditions, 74.11% of zinc was obtained. The kinetic data obtained was analyzed by the shrinking core model (SCM). A new SCM variant captured the kinetic data more appropriately. Based on this model, the activities of the reactants control the diffusion but the two concentrations affect the second order reaction rate or diffusion in both directions. At 75 °C, the R^2 values in the surface chemical reactions and diffusion were 0.78 and 0.89, respectively. Using the new model, however, the R^2 value 0.989 was obtained. The reaction orders with respect to $[H_2SO_4]$, $[NaNO_3]$, S/L ratio, and particle size were 1.603, 1.093, -0.9156 , and -2.177 , respectively. The activation energy for the dissolution was 29.23 kJ/mol.

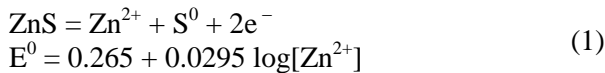
Keywords: Sulfide Ores, Leaching, Reaction Kinetics, Modeling.

1. Introduction

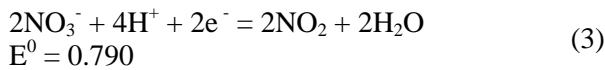
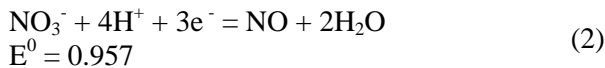
Sphalerite is the chief zinc ore, and is usually associated with galena, pyrite, and other sulfides along with calcite, dolomite, and fluorite. Froth flotation is a process for selectively separating the hydrophobic minerals from the hydrophilic ones [1]. Through the flotation process, the sphalerite concentrate produced has a zinc content greater than 50% [2]. The conventional RLE (roasting, leaching, and electro-winning) zinc production process has been in use since 1916. Currently, more than 85% of zinc is produced using this process [3]. However, due to the roasting stage, this method has numerous disadvantages such as high SO_2 production and high energy consumption (and hence, high production cost). To by-pass these problems, a number of researchers have been trying to develop alternative methods for preventing the production of SO_2 gas such as the direct leaching of sphalerite at the atmospheric pressure in the presence of

oxidants. In this context, numerous research efforts have been carried out using various oxidants like ferric ions [4], hydrogen peroxide [2], and ammonium persulfate [5] in acidic and alkaline solutions. However, most research works has been aimed at investigating the leaching of sulfides using nitric acid as the oxidant; the leaching processes using nitrates have not been sufficiently investigated, even though they oxidize as strongly as nitric acid [6]. Berdenhann [7] has investigated the nickel sulfide dissolution using ferric ions and sodium nitrate, as the oxidants, in acidic media. He has concluded that zinc extraction in the presence of sodium nitrate is higher than that in ferric ions. The copper recovery in the Cu_2S leaching using a sulfuric acid solution in sodium nitrate has been reported to be higher than 95% [6]. The oxidation of sphalerite in an acidic medium ($pH \leq 2$) is an electro-

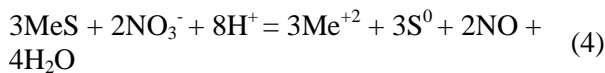
chemical process that releases zinc ions, and forms the elemental sulfur [8]:



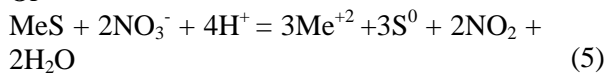
The oxidation of sodium nitrate in an acidic solution occurs according to the following equations [9]:



Comparison of Eq. 1 with the NaNO_3 redox reaction shows that the redox potential for sulfide/elemental sulfur is less than that for NaNO_3 . Therefore, the oxidation of sulfide to the elemental sulfur is possible. The leaching of a sulfide concentrate in an acidic solution in the presence of sodium nitrate can be expressed as follows [7]:



Or



Me: Divalent metal ions: Zn, Cu, etc.

In this work, the kinetics of the sphalerite dissolution by sodium nitrate in sulfuric acid was studied. The influences of the stirring speed,

particle size, acid concentration, sodium nitrate concentration, temperature, and liquid/solid (L/S) ratio were also investigated. Additionally, the kinetic data obtained was analyzed by the shrinking core model (SCM), and the best-fitting equation to the experimental data was determined.

2. Materials and method

A sphalerite concentrate sample obtained from Bama Lead and Zinc Complex in the Isfahan province in Iran was used. The sample was sieved to four-size fractions. The chemical analysis of each size fraction is presented in Table 1.

For the leaching experiments, a 1-L water glass recipient was used. The temperature was kept constant using a water bath. The calculated volumes of the H_2SO_4 and NaNO_3 solutions were added to the glass reactor, which was then heated to the desired temperature. Subsequently, a sample with a pre-determined weight was added to the reactor. At the specified time intervals, 1 mL of the solution was taken from the leach solution and diluted using distilled water. All the zinc analyses were carried out using an atomic absorption spectrophotometer (model Varian-AA240). The experimental conditions are shown in Table 2. Keeping the other parameters constant, the effect of each parameter on the dissolution rate was evaluated.

Table 1. Composition of sphalerite concentrate.

Particle size (μm)	Element (%)				
	Zn	Pb	Fe	S	SiO_2
-106+75	59.74	0.45	2.85	18.05	16.83
-75+53	58.73	0.49	1.94	18.58	17.34
-53+45	60.15	0.52	1.05	19.90	18.35
-45	59.85	0.43	2.95	18.14	18.97

Table 2. Parameter values for leaching of sphalerite.

Parameter	Values
Temperature ($^\circ\text{C}$)	45, 55, 65, 75*, 85
Acid concentration (M)	0.5, 1, 1.5, 2*, 2.5
Nitrate concentration (M)	0.1, 0.5, 1*, 1.5, 2
Particle size (μm)	-45, -53+45*, -75+53, -106+75
Solid to liquid ratio (g/L)	4, 8*, 12
Steering speed (rpm)	0, 200, 400*, 600

*Constant values used when effect of other parameters was investigated.

3. Effect of parameters on dissolution rate

3.1. Effect of solid/liquid ratio

The effect of the solid/liquid (S/L) ratio on the sphalerite dissolution was studied for three different solid/liquid (S/L) ratios (4, 8, and 12 g/L) at 75°C in a solution containing H_2SO_4 (2.0 M) and NaNO_3 (1.0 M). The stirring speed and

particle size were kept constant at 400 rpm and $-53 + 45 \mu\text{m}$, respectively. As shown in Figure 1, zinc extraction increased with a decrease in the amount of solid; this was caused by the increase in the acid available per unit of solid. To investigate the other leaching parameters, the 8 g/L S/L ratio was chosen.

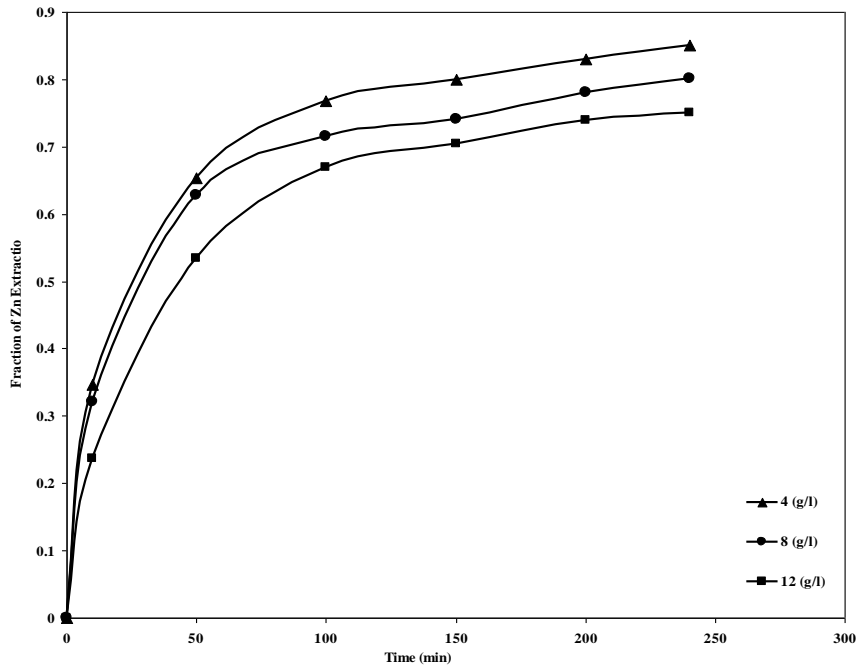


Figure 1. Effect of solid/liquid ratio on sphalerite dissolution.

3.2. Effect of particle size

To investigate the influence of the particle size on the dissolution rate, leaching experiments were carried out for different particle sizes ($-106 + 75$, $-75 + 53$, $-53 + 45$, and $-45 \mu\text{m}$), while the other parameters were kept constant. As it can be seen in Figure 2, the dissolution rate increased significantly with decrease in the particle size due

to the presence of the smaller particles, providing larger contact surface areas between the sphalerite and the leaching reagent. Zinc extraction decreased from 74.11 to 69% after 150 min, as the particle size increased from $-53 + 45$ to $-75 + 53 \mu\text{m}$. The other leaching parameters were analyzed using a $-53 + 45 \mu\text{m}$ particle size.

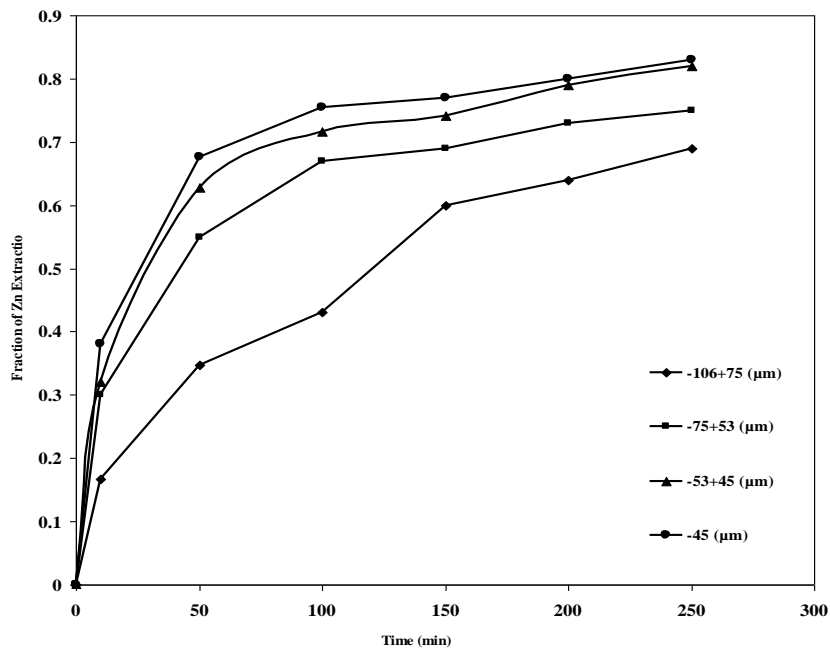


Figure 2. Effect of particle size on sphalerite dissolution.

3.3. Effect of stirring speed

The influence of the stirring speed on the sphalerite dissolution was studied at 0, 200, 400, and 600 rpm and 75 °C in a solution containing H₂SO₄ (2.0 M) and NaNO₃ (1.0 M). As shown in Figure 3, the stirring speed had an important effect on the dissolution of the sphalerite. The zinc recovered under similar experimental conditions, however, without agitation, was

approximately 30%. It was almost 74.11% when a 400 rpm stirring speed was induced, which shows that the rate of the sphalerite dissolution depends on the stirring speed. Hence, there is an indication that the reaction is controlled by the film diffusion. In analyzing the effects of the other parameters, 400 rpm was chosen as the optimal operating stirring speed.

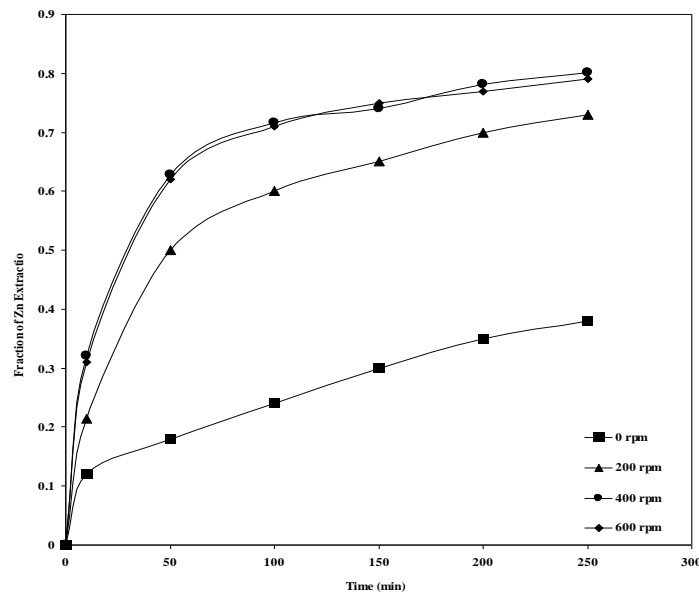


Figure 3. Effect of stirring speed on sphalerite dissolution.

3.4. Effect of temperature

To determine the influence of temperature, leaching experiments were performed at the five temperatures 45, 55, 65, 75, and 85 °C. The fixed laboratory parameters at this stage were the stirring speed of 400 rpm, sulfuric acid (2.0 M), sodium nitrate (1.0 M), particle size of -53 + 45

µm, and phase ratio of 8 g/L. With an increase in the temperature, the sphalerite dissolution rate increased. As it can be seen in Figure 4, after 150 min, with an increase in the temperature from 45 to 75 °C, the dissolution rate increased from 63.47 to 74.11%.

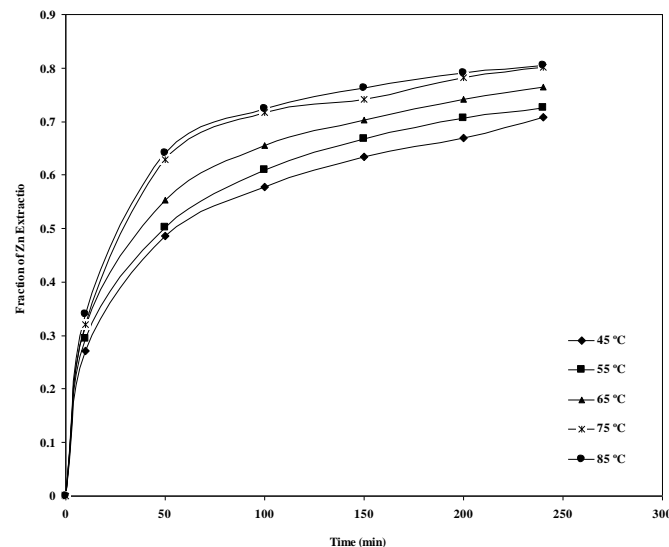


Figure 4. Effect of temperature on sphalerite dissolution.

3.5. Effect of H₂SO₄ concentration

The effect of the H₂SO₄ concentration on the sphalerite dissolution was studied for the 0.5, 1.0, 1.5, 2.0, and 2.5 M H₂SO₄ concentrations at 75 °C in a solution containing NaNO₃ (1.0 M). The results obtained are given in Figure 5. An increase in the H₂SO₄ concentration results in a moderate increase in the zinc extraction. However, at a high acid concentration (2.0 and 2.5 M), the effect is not significant. Zinc leaching increased from 47 to

74.11% after 150 min as the acid concentration was increased from 0.5 to 2.0 M. With an increase in the acid concentration to 2.5 M, the dissolution rate increased to 2.5%, ultimately reaching 76%. With an increase in the acid concentration, the hydrogen ion concentration in the leaching solution increased, raising the redox potential for the oxidant, and enhancing the dissolution rate.

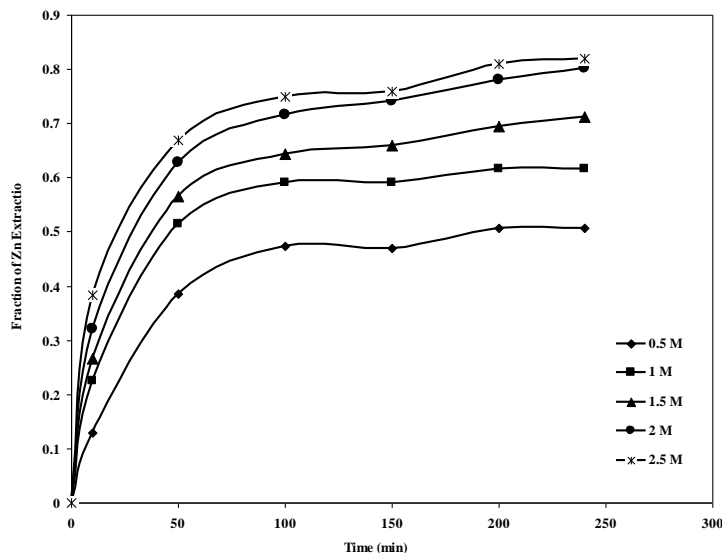


Figure 5. Effect of acid concentration on sphalerite dissolution.

3.6. Effect of NaNO₃ concentration

The effect of NaNO₃ concentration on the zinc extraction is shown in Figure 6. Experiments were carried out at the five different NaNO₃ concentrations 0.1, 0.5, 1.0, 1.5, and 2.0 M. The results obtained show that an increase in the oxidant concentration accelerates the sphalerite dissolution. At low concentrations of sodium nitrate, the sphalerite dissolution rate was very

weak, confirming that without the oxidant, the sphalerite dissolution did not occur.

The X-ray diffraction (XRD) analysis of the solid residue obtained from the leaching experiment is shown in Figure 7. As demonstrated, the elemental sulfur and sphalerite appear in the graph, which confirms that the elemental sulfur is formed during the leaching process.

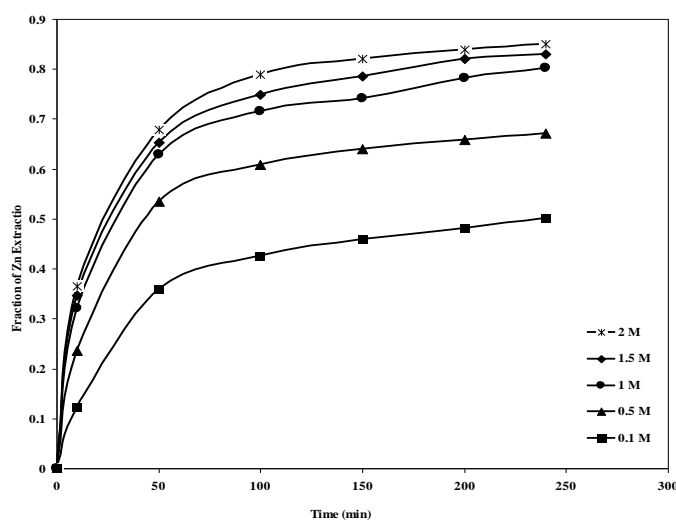


Figure 6. Effect of sodium nitrite concentration on sphalerite dissolution.

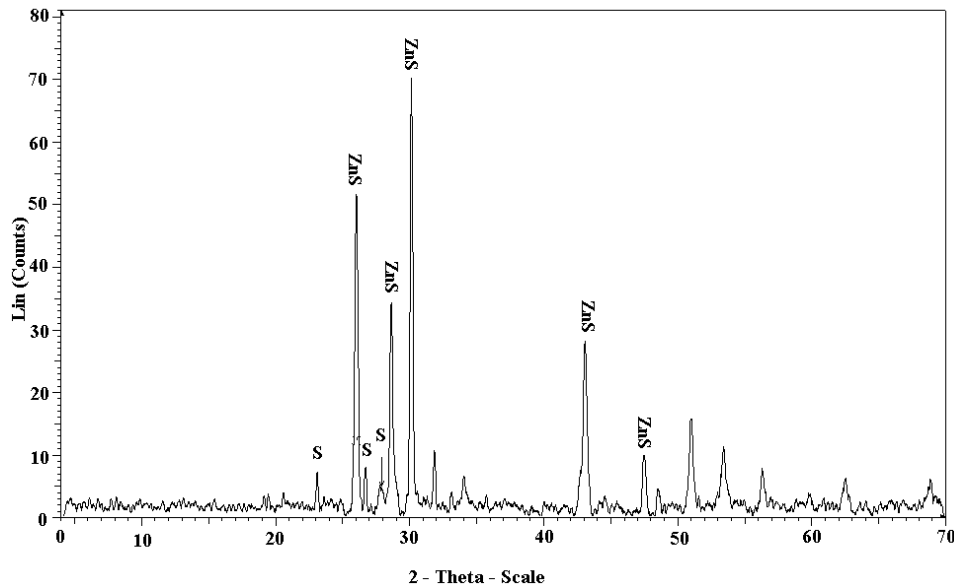
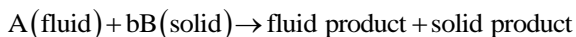


Figure 7. X-ray recordings of leach residue at optimum conditions.

4. Kinetic analysis

Leaching is a heterogeneous process, involving the mass transfer of the reactant and product ions. The dissolution of various mineral particles was investigated using different models. As the dissolution proceeds, the particles shrink with time until the total surface area of the particles diminishes, and the overall dissolution rate is reduced. If a product layer is formed around the particles, the dissolution process can be analyzed by SCM, though the model can be used even if there is no layer formation. Additionally, during the dissolution of the particles in some reactions, a loss of reagents or the exit of products may block the filling of pores with either impurity already present in the ore (clays, etc.) or re-precipitated leaching products. This leads to a “blocked-pore” kinetic model [10]. Similarly, the sphalerite dissolution in an acidic medium is a heterogeneous process, and most sulfide mineral leachings follow SCM [1]. According to this model, the reaction of the sphalerite can be expressed as follows:



The reaction rate is controlled by the following two equations.

When the resistance to diffusion through the product layer controls the reaction rate, the following equation expresses the dissolution rate [11, 12]:

$$1 - \frac{2}{3}X - (1-X)^{\frac{2}{3}} = \frac{2M_B DC_A}{P_B ar_0^2} t = K_d t \quad (6)$$

When the the reaction progress is unaffected by the presence of an ash layer, the reaction rate is proportional to the available surface of the unreacted core. In this case, the reaction rate is controlled by the surface chemical reactions. The following equation expresses the dissolution rate [11, 12]:

$$1 - (1-X)^{\frac{1}{3}} = \frac{K_C M_B C_A}{\rho_B ar_0} = K_r t \quad (7)$$

where X is the fraction reacted, K_C is the kinetic constant, M_B is the molecular weight of the solid, C_A is the concentration of the dissolved lixiviant, a is the stoichiometric coefficient of the reagent in the leaching reaction, r_0 is the initial radius of the solid particle, t is the reaction time, ρ_B is the the solid density, and K_r is the rate constant.

Numerous researchers who have investigated the kinetics of the sphalerite dissolution process under various conditions have pointed out that it is either a reaction- or diffusion-controlled process [13, 14]. However, in a few cases, neither of the two equations mentioned has been able to explain the sphalerite dissolution rate.

Bobeck [15] used Eq. 8, which is included in both Eqs. 6 and 7:

$$\left[1 - (1-X)^{\frac{1}{3}} \right] + B \left[1 - \frac{2}{3}X - (1-X)^{\frac{2}{3}} \right] = Kt \quad (8)$$

where
 $B = K_r/K_d$.

Dehghan et al. [16] have reviewed the sphalerite dissolution kinetics in an acidic ferric chloride solution and concluded that the sphalerite leaching is not appropriately captured by Eqs. 6 and 7; they used a new type of SCM, which provided a better fit to the kinetic data. Moreover, Dehghan et al. have found that both the interfacial transfer and diffusion through the product layer affect the reaction rate. The model equation is given as:

$$\frac{1}{3} \ln(1-X) + \left[(1-X)^{-\frac{1}{3}} - 1 \right] = K_m t \quad (9)$$

Compared to the models presented above, a new variant of SCM proposed by Dickinson and Heal [17] has provided a better expression for the sphalerite leaching using the kinetic data for sodium nitrate in sulfuric acid. According to this model, which is a more complete type of the diffusion-control model (Eq. 6), both the solid and acid concentrations have a role in controlling the

reaction rate, and diffusion occurs in two directions. An equation for this model is given as follows:

$$\frac{1}{5}(1-X)^{-\frac{5}{3}} - \frac{1}{4}(1-X)^{-\frac{4}{3}} + \frac{1}{20} = K_p t \quad (10)$$

$$K_p = \frac{DV_m C_{0A} C_{0B}}{r_0^2}$$

Where, K_p is a kinetic constant, V_m is the volume of the produced layer, D is the diffusion coefficient, and C_0 is the concentration of the penetrating species at the surface (A, solid and B, fluid).

In Figure 8, $\frac{1}{5}(1-X)^{-\frac{5}{3}} - \frac{1}{4}(1-X)^{-\frac{4}{3}} + \frac{1}{20}$ has been plotted vs. time at different temperatures. The slope of this line is the specified kinetic constant.

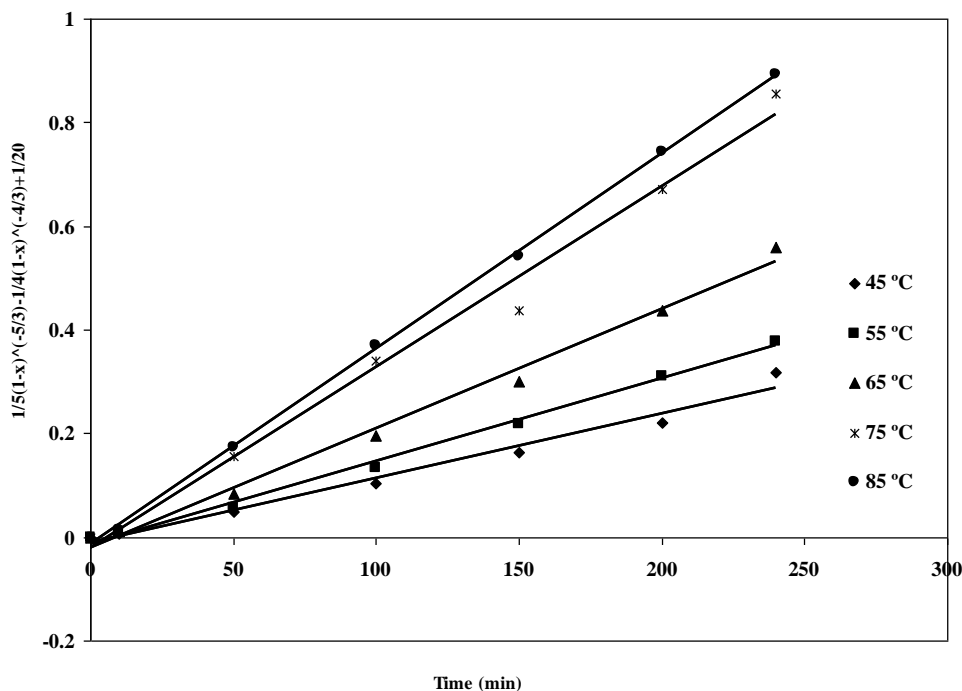


Figure 8. Variation in $\frac{1}{5}(1-X)^{-\frac{5}{3}} - \frac{1}{4}(1-X)^{-\frac{4}{3}} + \frac{1}{20}$ with time at various temperatures.

As it can be seen in Table 3, the popular modes of SCM (Eqs. 6 and 7) were compared to the new mode (Eq. 10). According to the results given in this table, SCM with diffusion through the product layer, compared to the chemical reaction-

controlled model, showed a better fit to the data but the new SCM mode suggested by Dikenson provided an even better fit due to a more linear relationship between the left side of Eq. 10 and time.

Table 3. Correlation coefficient values for different temperatures.

Temperature (°C)	Surface reaction	Diffusion	New variant of SCM
	R ²	R ²	R ²
45	0.8421	0.9590	0.9809
55	0.8366	0.9508	0.9952
65	0.8210	0.9374	0.9921
75	0.7833	0.8924	0.9898
85	0.7718	0.8804	0.9994

The temperature-dependence of the reaction rate constant can be determined through the Arrhenius equation [18]:

$$K_p = A \exp\left(\frac{-E_a}{RT}\right) \quad (11)$$

where A is the frequency factor, E_a is the activation energy of the reaction, R is the universal gas constant, and T is the absolute

temperature. With respect to Eq. 11, if the plot of ln k_p vs. 1/T is drawn, the slope of the line is E_a/R. If this value is multiplied by R, the activation energy value is obtained. As it can be seen in Figure 9, the slope of the line is 3.5052, and we obtained the activation energy value of 29.23 kJ/mol.

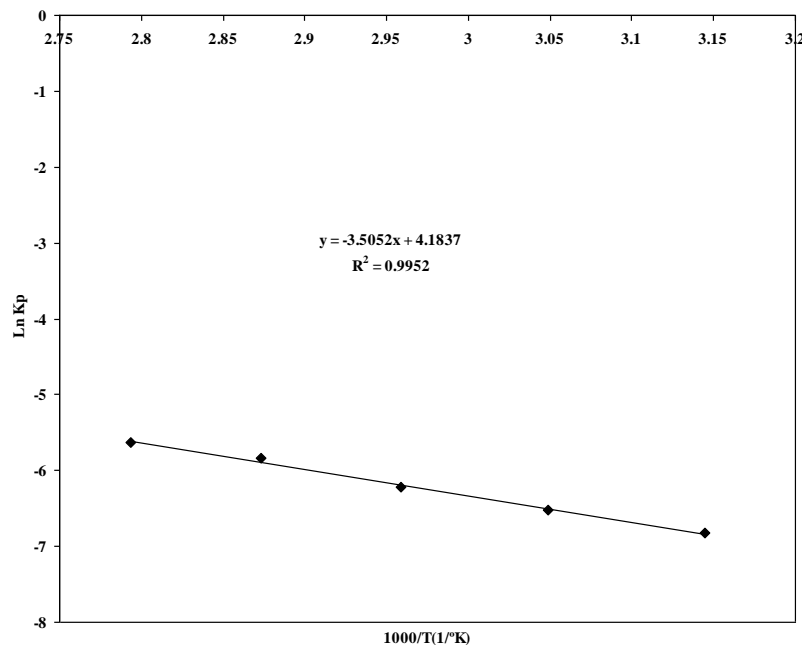


Figure 9. Arrhenius plot of data presented in Figure 8.

The activation energy for a diffusion-controlled process is different from that for a process controlled by a chemical reaction. The activation energy for a process controlled by a diffusion mechanism is 4-12 kJ/mol; for a chemical reaction mechanism, the activation energy is greater than 40 kJ/mol [19]. However, other studies have offered the following different results: the activation energies of 2-5 and 12-26 kJ/mol for the diffusion-controlled process, and 40-80 kJ/mol for the process controlled by a chemical reaction [19-21]. Babu [5] has obtained an activation energy of 41 kJ/mol for the diffusion-controlled process, and Dehqan [16] has obtained it to be 49.2 kJ/mol. In addition, Adabayo [14] and Arawi [22] have, respectively, obtained the activation

energies of 28 and 16 kJ/mol for two processes controlled by a chemical reaction.

Hence, the magnitude of the activation energy cannot determine the control mechanism of the process; it can only be used as a guide for determining the leaching process.

Therefore, we can conclude that if the activation energy is less than 30 kJ/mol, the process is not controlled by a chemical reaction, and it is more likely to be controlled by diffusion. Moreover, in the diffusion-controlled process, there is a close correlation between the stirring speed and the reaction rate caused by the thickness reduction of the product layer. Thus three factors confirm that our process is controlled by a diffusion mechanism, as follow: its low activation energy (29.23 kJ/mol), the correlation between the

stirring speed and Zn extraction (Figure 5), and the fit of Eq. 10 to the experimental data. In the next stage of our experiments, the reaction order with respect to the sulfuric acid and sodium nitrate concentrations, particle size, and S/L ratio was determined. $\ln k_p$ vs. $\ln[H_2SO_4]$ was plotted (Figure 10). The slope of the line obtained conveys the reaction order with respect to the sulfuric acid concentration, and is proportional to $[H_2SO_4]^{1.6032}$, with a correlation coefficient of 0.986.

$\ln k_p$ vs. $\ln[NaNO_3]$ was plotted (Figure 11). The reaction order with respect to sodium nitrate was

1.093, and the slope of the line obtained is proportional to $[NaNO_3]^{1.093}$.

$\ln k_p$ vs. $\ln[S/L]$ was plotted (Figure 12); it can be used to determine the reaction order with respect to the S/L ratio. The reaction order was found to be -0.9156 , and the slope of the line obtained is proportional to $(S/L)^{-0.9156}$.

Finally, as it can be seen in Figure 13, the reaction order with respect to the particle size was -2.1777 , and the slope of the line obtained is proportional to $[Size]^{-2.1777}$.

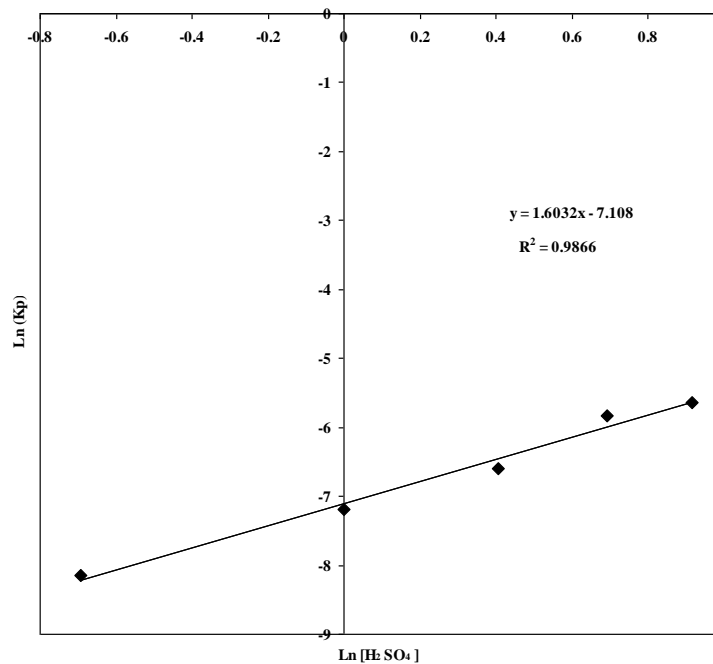


Figure 10. Determination of reaction order with respect to $\ln[H_2SO_4]$.

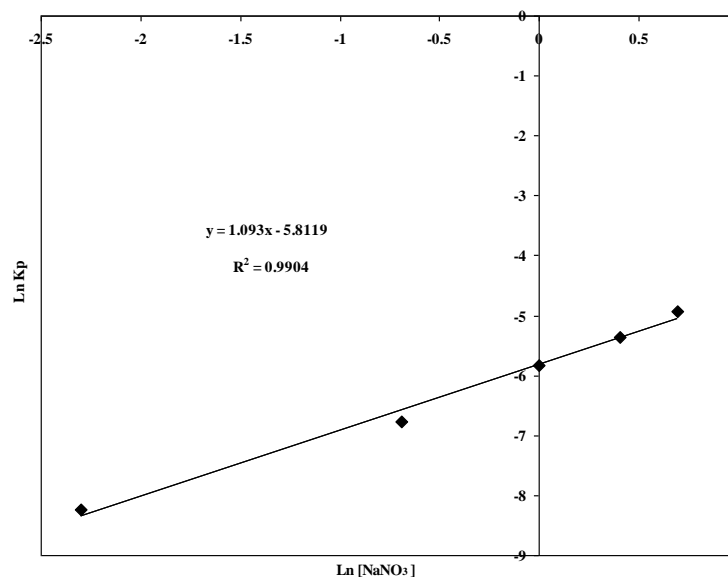


Figure 11. Determination of reaction order with respect to $\ln[NaNO_3]$.

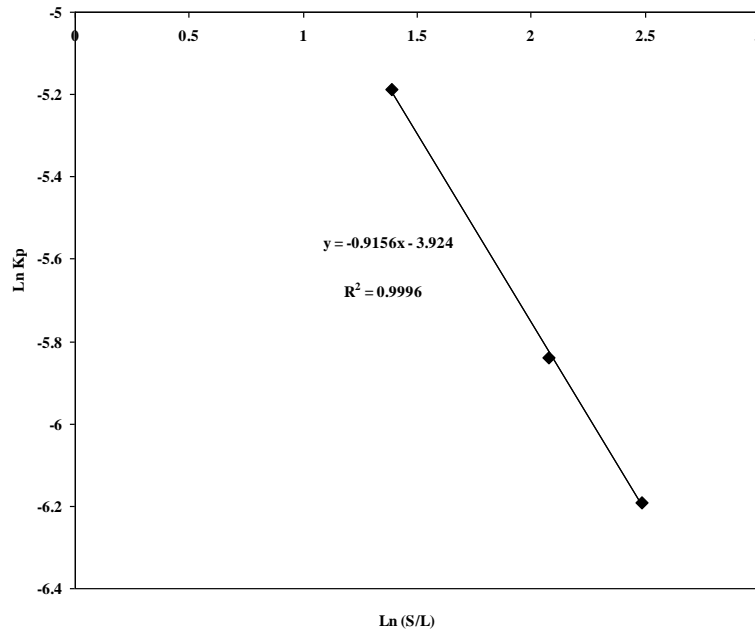


Figure 12. Determination of reaction order with respect to ln[S/L].

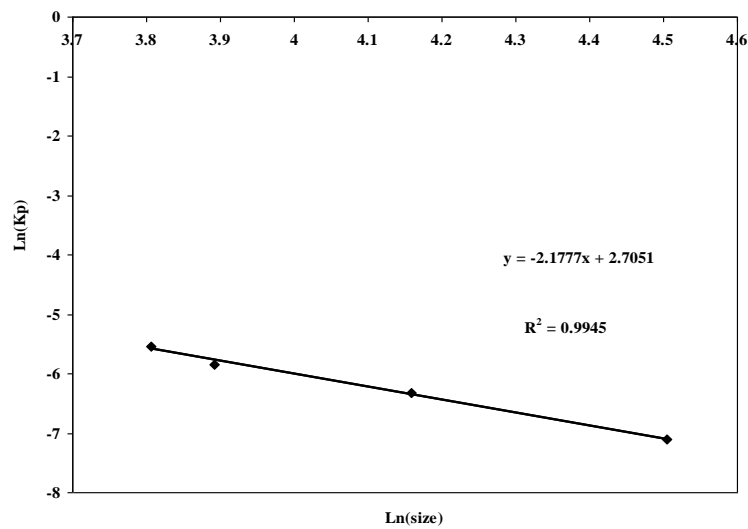


Figure 13. Determination of reaction order with respect to ln[Size].

5. Dissolution rate equation

By determining the activation energy of the dissolution process and the reaction orders with respect to the experimental conditions, the following equation could be used to describe the kinetics of the sphalerite dissolution by sodium nitrate in sulfuric acid:

$$\frac{1}{5}(1-X)^{-\frac{5}{3}} - \frac{1}{4}(1-X)^{-\frac{4}{3}} + \frac{1}{20} = K_0 [H_2SO_4]^{1.6032} [NaNO_3]^{1.093} (r_0)^{-2.1777} \left(\frac{S}{L}\right)^{-0.9156} \exp\left(\frac{-29233}{RT}\right) t$$

As shown in Figure 14, plotting

$$[H_2SO_4]^{1.6032} [NaNO_3]^{1.093} (r_0)^{-2.1777} \left(\frac{S}{L}\right)^{-0.9156} \exp\left(\frac{-29233}{RT}\right) t$$

vs.

$$\frac{1}{5}(1-X)^{-\frac{5}{3}} - \frac{1}{4}(1-X)^{-\frac{4}{3}} + \frac{1}{20}$$

gives a k_0 value of 829423.

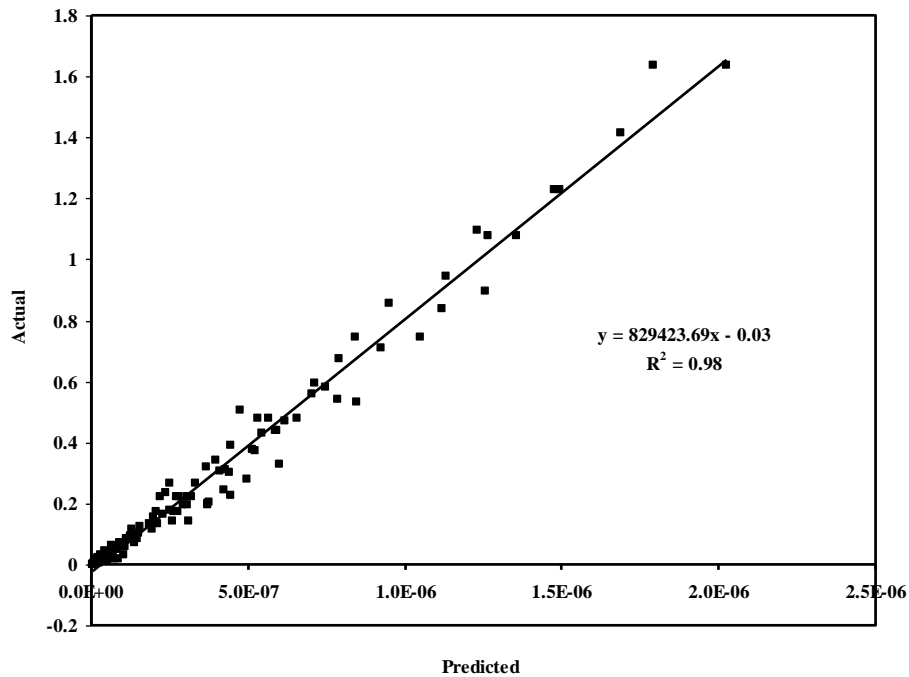


Figure 14. Plot of Arrhenius constant $([H_2SO_4]^{1.6032} [NaNO_3]^{1.093} (r_0)^{-2.1777} \left(\frac{S}{L}\right)^{-0.9156} \exp\left(\frac{-29233}{RT}\right) t$ vs. $\frac{1}{5}(1-X)^{-\frac{5}{3}} - \frac{1}{4}(1-X)^{-\frac{4}{3}} + \frac{1}{20}$.

The extraction rates obtained under the experimental conditions and those calculated by the model were compared. Under the optimum dissolution conditions, which were determined to be H_2SO_4 (2.0 M), $NaNO_3$ (1.0 M), 75 °C, 8 g/L S/L ratio, 150 min leaching time, and $-45 + 53 \mu m$ particle size, the extracted zinc was calculated using the following equation:

$$\frac{1}{5}(1-X)^{-\frac{5}{3}} - \frac{1}{4}(1-X)^{-\frac{4}{3}} + \frac{1}{20} = 82.9 \times 10^4 [2]^{1.6032} [1]^{1.093} (49)^{-2.1777} (8)^{-0.9156} \exp\left(\frac{-29233}{8.314 * 348}\right) (150)$$

According to the equation, the extracted zinc, X, was 75.3%, while the zinc extracted under the experimental conditions was 74.11%. This demonstrates a significant correlation between the experimental and calculated values.

6. Conclusions

- In this work, the kinetics of the sphalerite concentrate leaching by sulfuric acid and sodium nitrate were studied. The effects of the experimental parameters such as the temperature, sulfuric acid and sodium nitrite concentrations, stirring speed, particle size, and S/L ratio were analyzed.

- The dissolution rate increased with increase in the sulfuric acid and sodium nitrite concentrations and temperature. However, it decreased with increase in the particle size and S/L ratio. Moreover, the stirring speed had a significant effect on the leaching rate.

- The optimum leaching conditions were determined to be: size, $(-75 + 53) \mu m$; $[NaNO_3]$, 1 mol/L; $[H_2SO_4]$, 2 mol/L; T, 75 °C; and S/L, 8 g/L. Under these conditions, 74.11% of zinc was extracted in 150 min.

- The kinetic data was analyzed by SCM. The new SCM variant fits the kinetic data more appropriately.

- The reaction orders with respect to the H_2SO_4 and $NaNO_3$ concentrations, S/L ratio, and particle size were found to be 1.603, 1.093, -0.9156 , and -2.177 , respectively.

- The activation energy was calculated to be 29.23 kJ/mol.

- The dissolution rate can be expressed by Eq. 4, which represents a semi-empirical mathematical model.

Acknowledgments

The authors are grateful to the Tarbiat Modares and Tehran Universities for supporting in this research work.

References

- [1]. Uçar, G. (2009). Kinetics of sphalerite dissolution by sodium chlorate in hydrochloric acid. *Hydrometallurgy* 95: 39-43.
- [2]. Aydoğan, S. (2006). Dissolution kinetics of sphalerite with hydrogen peroxide in sulphuric acid medium. *Chemical Engineering Journal*. 123: 65-70.
- [3]. Zhi, F., Qing, J. and Wang, C. (2013). Atmospheric oxygen-rich direct leaching behavior of zinc sulphide concentrate. *Trans. Nonferrous Met. Soc. China*. 23: 3780-3787.
- [4]. Akcil, A. and Ciftci, H. (2002). A study of the selective leaching of complex sulfides from the Eastern Black Sea Region, Turkey, *Minerals Engineering*. 15: 457-459.
- [5]. Babu, M.N., Sahu, K.K. and Pandey, B.D. (2002). Zinc recovery from sphalerite concentrate by oxidative leaching with ammonium, sodium and potassium persulfates. *Hydrometallurgy*. 64: 119-129.
- [6]. Rajko, Z. and Vracar, A. (2003). Leaching of copper (I) sulphide by sulphuric acid solution with addition of sodium nitrate, *Hydrometallurgy*. 70: 143-151.
- [7]. Berdenhan, R. and Vanvuuren, C. (1999). Technical note the leaching behavior of a nickel concentrate in an oxidative sulphuric acid solution. *Minerals Engineering*. 12: 687-692.
- [8]. Pecina, T., Telhma, F. and Pedro, C. (2008). Leaching of a zinc concentrate in H₂SO₄ solutions containing H₂O₂ and complexing agents, *Minerals Engineering*. 21: 23-30.
- [9]. Miroslav, D. and Sokić, A. (2009). Kinetics of chalcopyrite leaching by sodium nitrate in sulphuric acid, *Hydrometallurgy*. 95: 273-279.
- [10]. Shafaei, S.Z. (1996). Hydrometallurgical processing of angouran oxidized zinc. PhD thesis, the University of Leeds, pp. 142-200.
- [11]. Zhenghui, W., Dreisinger, D., Urchb, H. and Fassbender, S. (2014). The kinetics of leaching galena concentrates with ferric methane sulfonate solution. *Hydrometallurgy*. 142: 121-130.
- [12]. Xiong, L.Z., Lan, Z., Shao, Y., Xiong, F. and Chenc, Y.C. (2014). Leaching and kinetic modeling of calcareous bornite in ammonia ammonium sulfate solution with sodium persulfate. *Hydrometallurgy*. 144: 86-90.
- [13]. Rath, P.C., Paramguru, R.K. and Jena, P.K. (1981). Kinetics of dissolution of zinc sulphide in aqueous ferric chloride solution. *Hydrometallurgy*. 6: 219-225.
- [14]. Adebayo, A.O., Ipinmoroti, K.O. and Ajayi, O. (2006). Leaching of Sphalerite with Hydrogen Peroxide and Nitric Acid Solutions. *Minerals & Materials Characterization & Engineering*. 5 (2): 167-177.
- [15]. Bobeck, G.E. and Su, H. (1985). The kinetics of dissolution of sphalerite in ferric chloride solution. *Metall. Trans. B* 16B: 413-424.
- [16]. Dehghan, R. and Kolahdoozan, M. (2008). Leaching and kinetic modelling of low-grade calcareous sphalerite in acidic ferric chloride solution, *Hydrometallurgy*. 96: 275-282.
- [17]. Dickinson, C.F. and Heal, G.R. (1999). Solid-liquid diffusion controlled rate equations. *Thermochim. Acta* 340-341: 89-103.
- [18]. Safarzadeh, M., Moradkhani, D. and Ojaghi, M., (2008). Kinetics of sulfuric acid leaching of cadmium from Cd-Ni zinc plant residues, *Journal of Hazardous Materials*. 163: 880-890.
- [19]. Habashi, F. (1980). *Principles of Extractive Metallurgy*, second ed., Gordon and Breach Science Publ., New York.
- [20]. Abdel-Aal, E.A. and Rashad, M.M., (2004). Kinetic study on the leaching of spent nickel oxide catalyst with sulfuric acid, *Hydrometallurgy*. 74: 189-194.
- [21]. Romankiw, L.T. and De Bruyn, P.L. (1963). Kinetics of dissolution of zinc sulfide in aqueous sulfuric acid. In: Wadsworth, M., Davis, F.T. (Eds.), *Unit Processes in Hydrometallurgy*, 62 Dallas, TX.
- [22]. Harvey, J.T., Tai, Y. and Paterson, J.G. (1993). A kinetic investigation into the pressure oxidation of sphalerite from a complex concentrate, *Mineral Engineering*. 6: 949-967.

سینتیک انحلال اسفالریت در محلول اسیدسولفوریک در حضور نیترات سدیم

مسعود حسنى، سید محمد جواد کلینی و احمد خدادادی*

بخش مهندسی معدن، دانشگاه تربیت مدرس، ایران

ارسال ۲۰۱۴/۷/۱، پذیرش ۲۰۱۵/۵/۴

* نویسنده مسئول مکاتبات: akdarban@modares.ac.ir

چکیده:

در پژوهش حاضر، استخراج روی از کنسانتره اسفالریت در محلول اسید سولفوریک و در حضور اسید نیتریک به‌عنوان اکسیدان مورد بررسی قرار گرفت. پارامترهای تأثیرگذار نظیر دما، غلظت اسیدسولفوریک، غلظت اسید نیتریک، دور همزن، اندازه ذرات و نسبت جامد به مایع مورد بررسی قرار گرفتند از نتایج حاصل مشخص شد که نرخ انحلال با افزایش غلظت اسیدسولفوریک و اسید نیتریک و نیز دما افزایش می‌یابد و با افزایش اندازه ذرات و نسبت جامد به مایع کاهش می‌یابد. در نهایت، در شرایط بهینه، میزان استخراج روی برابر ۷۴/۱۱٪ به دست آمد. سینتیک فرآیند نیز توسط مدل هسته‌ی کوچک شونده مورد آنالیز قرار گرفت. یک نوع جدید از این مدل بهترین تطابق را با داده‌های آزمایشگاهی نشان داد. بر مبنای این مدل اکتیویته‌ی حلال و جسم جامد هر دو بر نرخ انحلال تأثیر می‌گذارند و دیفیوژن در دو جهت بر فرآیند تأثیر می‌گذارد. در دمای ۷۵ درجه سانتی‌گراد میزان R^2 برای دو مکانیسم واکنش شیمیایی و دیفیوژن به ترتیب برابر با ۰/۷۸ و ۰/۸۹ به دست آمد اما برای مدل جدید برابر ۰/۹۸۹ به دست آمد. همچنین مرتبه‌های واکنش با توجه به غلظت‌های اسیدسولفوریک، نیترات سدیم، نسبت جامد به مایع و اندازه ذرات به ترتیب برابر با ۰/۶۰۳، ۱/۰۹۳، ۰/۹۱۵۶- و ۲/۱۷۷- به دست آمدند. انرژی اکتیواسیون نیز برابر ۲۹/۲۳ کیلوژول بر مول به دست آمد.

کلمات کلیدی: کانه‌های سولفیدی، لیچینگ، سینتیک فرآیند، مدل‌سازی.
